



OPEN ACCESS

EDITED BY

Axel Schambach,
Hannover Medical School, Germany

REVIEWED BY

Sadhak Sengupta,
IN8Bio, Inc., United States
Zibing Wang,
Henan Provincial Cancer Hospital, China

*CORRESPONDENCE

Eva Rettinger
✉eva.rettinger@icloud.com
Laura M. Moser
✉moser@med.uni-frankfurt.de

RECEIVED 24 August 2024

ACCEPTED 09 January 2025

PUBLISHED 03 February 2025

CITATION

Moser LM, Heim C, Koschade SE, Wendel P, Bozkurt S, Harenkamp S, Kreyenberg H, Merker M, Münch C, Gradhand E, Vogler M, Ullrich E, Bönig H, Klusmann J-H, Bader P, Wels WS and Rettinger E (2025) CAR-CIK vs. CAR-T: benchmarking novel cytokine-induced killer cells as solid tumor immunotherapy in ErbB2+ rhabdomyosarcoma. *Front. Immunol.* 16:1485817. doi: 10.3389/fimmu.2025.1485817

COPYRIGHT

© 2025 Moser, Heim, Koschade, Wendel, Bozkurt, Harenkamp, Kreyenberg, Merker, Münch, Gradhand, Vogler, Ullrich, Bönig, Klusmann, Bader, Wels and Rettinger. This is an open-access article distributed under the terms of the [Creative Commons Attribution License \(CC BY\)](https://creativecommons.org/licenses/by/4.0/). The use, distribution or reproduction in other forums is permitted, provided the original author(s) and the copyright owner(s) are credited and that the original publication in this journal is cited, in accordance with accepted academic practice. No use, distribution or reproduction is permitted which does not comply with these terms.

CAR-CIK vs. CAR-T: benchmarking novel cytokine-induced killer cells as solid tumor immunotherapy in ErbB2+ rhabdomyosarcoma

Laura M. Moser^{1,2,3,4,5*}, Catrin Heim¹, Sebastian E. Koschade^{3,4,5,6,7}, Philipp Wendel^{2,3,8,9}, Süleyman Bozkurt⁷, Sabine Harenkamp¹⁰, Hermann Kreyenberg^{1,2}, Michael Merker^{1,2}, Christian Münch^{4,7,11}, Elise Gradhand¹², Meike Vogler^{3,4,13}, Evelyn Ullrich^{2,3,4,5,8}, Halvard Bönig^{10,14}, Jan-Henning Klusmann^{2,3,4,5}, Peter Bader^{1,2,3,4,5}, Winfried S. Wels^{3,4,15} and Eva Rettinger^{1,2,3,4,5*}

¹Division for Stem Cell Transplantation and Immunology, Department of Pediatrics, Goethe University Frankfurt, Frankfurt am Main, Germany, ²Department of Pediatrics, Goethe University Frankfurt, Frankfurt am Main, Germany, ³German Cancer Consortium (DKTK), partner site Frankfurt/Mainz, Frankfurt am Main, Germany, ⁴Frankfurt Cancer Institute (FCI), Goethe University, Frankfurt am Main, Germany, ⁵Universitäres Centrum für Tumorerkrankungen (UCT), Frankfurt am Main, Germany, ⁶Department of Medicine, Hematology/Oncology, Goethe University Frankfurt, Frankfurt am Main, Germany, ⁷Institute of Biochemistry II, Faculty of Medicine, Goethe University, Frankfurt am Main, Germany, ⁸Experimental Immunology & Cell Therapy, Department of Pediatrics, Goethe University, Frankfurt am Main, Germany, ⁹Institute for Organic Chemistry and Biochemistry, Technical University of Darmstadt, Darmstadt, Germany, ¹⁰Department of Cellular Therapeutics/Cell Processing, Institute for Transfusion Medicine and Immunotherapy, Goethe University, Frankfurt am Main, Germany, ¹¹Cardio-Pulmonary Institute, Frankfurt am Main, Germany, ¹²Department of Pediatric and Perinatal Pathology, Dr. Senckenberg Institute of Pathology, Goethe-University Frankfurt, Frankfurt am Main, Germany, ¹³Institute for Experimental Pediatric Hematology and Oncology, Goethe University, Frankfurt am Main, Germany, ¹⁴Division of Hematology, Department of Medicine, University of Washington, Seattle, WA, United States, ¹⁵Georg-Speyer-Haus, Institute for Tumor Biology and Experimental Therapy, Frankfurt am Main, Germany

Introduction: CAR-T cell therapy, though successful in hematologic malignancies, faces challenges in solid tumors due to limitations of autologous T cells. Cytokine-induced killer (CIK) cells can be given safely across allogeneic barriers and constitute alternative effector cells generated from healthy donors. CIK cells are a heterogenous population of predominantly T cells with a mixed natural killer (NK) phenotype and combine non-MHC-restricted cytotoxicity with potent anti-tumor capacity of the adaptive immune system. Here, we characterize and compare efficacy, phenotypic subpopulations and modes of action of CAR-CIK cells and conventional CAR-T cells from same-donor samples in ErbB2+ rhabdomyosarcoma (RMS).

Methods: To benchmark CAR-CIK against conventional CAR-T cells, effector cells were generated from same-donor samples and lentivirally transduced with a second generation CD28-CD3 ζ CAR. Effector subpopulations and their dynamics upon target cell exposure were phenotypically characterized by flow cytometry. Efficacy was assessed in human ErbB2+ RMS cancer cell lines and

primary patient samples *in vitro* and *ex vivo* using cytotoxicity and spheroid co-incubation assays. Modes of action were assessed by comparing cytokine secretion profiles using bead-based multiplexed flow cytometry and by liquid chromatography mass spectrometry whole cell proteomics. Finally, we used an *in vivo* model of RMS mimicking minimal metastatic residual disease to compare anti-tumor potency of CAR-CIK vs. CAR-T cells and to assess their target organ infiltration.

Results: *In vitro* assays demonstrated superior cytotoxicity of CAR-CIK cells against RMS cell lines and primary tumor samples. Long-term co-incubation with tumor spheroids led to expansion of CAR-CIK cells and enrichment of CD3+CD56+ TNK cells. CAR-CIK cell cytokine signature showed significantly increased secretion of effector molecules like interferon- γ , perforin and granulysin, and lower secretion of Th2 cytokines IL-2, IL-4 and IL-10. Whole cell proteomics showed corresponding upregulation of chemokine signaling and NK-cytotoxicity pathways in CAR-CIK cells. In NSG mice xenografted with ErbB2+ RMS, a single injection of either CAR-effector cells strongly impeded metastatic tumor development and significantly improved survival.

Conclusion: Our results demonstrate that CAR-CIK cells are at least equipotent to CAR-T cells. Combined with their favorable safety profile and allogeneic applicability, these findings position CAR-CIK cells as promising immune effectors for solid tumors.

KEYWORDS

cytokine-induced killer cells (CIK), CAR-T, rhabdomyosarcoma, solid tumors, ERBB2

1 Introduction

Adoptive cellular therapies have emerged as a powerful treatment option for hematological malignancies. In B cell neoplasias, chimeric antigen receptor (CAR) therapy has shown spectacular results and several CAR-T cell products have now been approved and adopted into standard therapy (1–5). However, the success of CAR-T cell therapy has so far been limited when applied to solid cancers (6). This can be attributed to several factors including antigen heterogeneity, antigen escape, high tumor burden, poor accessibility of solid tumors as well as an immunosuppressive tumor microenvironment (TME) (6–9). Low efficacy of CAR-T cell therapy can further be caused by fundamental limitations of autologous T cells (6, 10, 11). Immunosuppressive factors of the tumor can induce T cell dysfunction and (numerous) lines of previous therapy negatively affect the number of autologous T cells and their quality as starting material for CAR-T cell production. T cells from a (partially) human-leukocyte antigen (HLA)-matched healthy donor could overcome these issues but can be associated with lethal Graft-versus-Host Disease (GvHD) outside the setting of allogeneic hematopoietic stem cell transplantation (allo-HSCT) (10, 12). Although additional genetic manipulations can mitigate the risk of GvHD, they also generate higher costs, induce new genetic alterations and compromise T cell intrinsic tumor recognition via the T cell

receptor (10). Alternative CAR-effector cells from healthy donors could help overcome these problems (9, 10, 12–14).

Cytokine-induced killer (CIK) cells have demonstrated efficacy and an excellent safety profile in clinical trials, even across HLA barriers in an allogeneic setting (14–20). They exert potent anti-tumor capacity against various hematological and solid malignancies (15, 21). CIK cells represent a heterogeneous T cell population with a mixed natural killer (NK) cell phenotype and combine adaptive T cell-mediated with major-histocompatibility (MHC)-unrestricted activity of the innate immune system. While the CD3+CD56+ TNK cell subset within CIK cells shares some features with invariant NKT (iNKT) (20–24) and $\gamma\delta$ T cells (25, 26), they are a distinct population with variable, mostly $\alpha\beta$ T cell receptors (TCRs) arising from CD3+ T cells (27–35). CIK cells are easily generated from peripheral blood mononuclear cells (PBMCs), expanded by *in vitro* cytokine addition and can be successfully engineered to express CARs (14, 15, 18, 36–38). However, these novel effector cells have not yet been directly benchmarked against conventional CAR-T cells, and their comparative efficacy remains unknown.

We chose advanced pediatric rhabdomyosarcoma (RMS) as a solid tumor model to comparatively assess CIK versus conventional T cells for CAR-engineering. In RMS, new treatment options and medical advances have not translated into better outcomes and

there is a high medical need to develop alternative therapies (39). Several types of sarcoma express ErbB2 (HER2) at low levels, rendering this receptor tyrosine kinase a potential target for immunotherapy (40). First clinical evaluations of ErbB2-directed CAR-T cells for sarcomas have proven the safety and feasibility of this approach but had limited efficacy (41–43).

We have previously shown that ErbB2-specific CAR-CIK cells mediate strong and specific activity against RMS (34, 44). Here, we present the first comprehensive comparative efficacy analysis *in vitro* and *in vivo* of CAR-CIK versus CAR-T cells with equal CAR-expression from same-donor samples targeting ErbB2 in RMS, including a thorough phenotypic characterization of these distinct CAR-effector cells. Using established RMS cell lines and primary samples from patients with metastatic disease, we demonstrate increased cytolytic activity of CAR-CIK cells *in vitro* and equipotency *in vivo*. Assessment of cytokine signatures and whole cell proteomics uncovered marked differences in the mechanisms of action of CAR-T and CAR-CIK cells, with the latter exerting their effects predominantly through NK cell-like cytotoxic pathways and related effector molecules. Given the limitations of autologous CAR-T cells, these findings position CAR-CIK cells as promising immune effectors for new cellular therapies in solid tumors.

2 Materials and methods

2.1 Primary RMS

Primary RMS samples were obtained from two pediatric RMS patients after written informed consent of their legal guardians in accordance with the Declaration of Helsinki. The ethics review board of the Goethe University (Frankfurt, Germany) approved the biomaterial usage (SPO-04-2015). H1 samples were from a cutaneous lesion of a progressing alveolar Pax3-FOXO1 fusion-positive RMS, H9 samples were from pleural metastases of an embryonal fusion-negative RMS. Both primary RMS samples were cultivated in DMEMHighGlucoseHepesGlutaMAX (ThermoFisher) supplemented with 10% FBS, 1% Penicillin/Streptomycin and 1% sodium-pyruvate.

2.2 Lentiviral particles and transduction of cell lines

GFP/luciferase-expressing as well as mCherry/luciferase-expressing cells were produced by lentiviral transduction using the pSIEW-luc2 (45) and pLenti_fLuc_mCherry plasmids and were enriched by fluorescence-activated cell sorting (sorting for GFP+ or mCherry+ cells, respectively) using a FACSAria II instrument (BD Biosciences).

2.3 Generation of parental and ErbB2-CAR-CIK and CAR-T cells

PBMCs from healthy volunteer donors were used as a source for CIK and T cells with a minimum of three independent donors for all

in vitro experiments (range 3–5). PBMCs were collected via standard density gradient separation using Histopaque-1077 (Sigma-Aldrich) after informed consent had been provided. The study and biomaterial usage were approved by the Ethics Review Board of the Medical Faculty of the University Hospital Frankfurt (Main), Germany (Nr. 413/15). T cells were isolated from PBMCs using the EasySep™ Human T cell isolation kit (StemCell) according to the manufacturer's instructions and cultivated in RPMI 1640 medium with GlutaMAX with 10% FBS, 2 mM L-Glutamine (ThermoFisher), 25 mM Hepes (ThermoFisher) and 50 μM 2-mercapto-ethanol containing 100 U/mL human IL-2 (Novartis). T cells were seeded in 48-well plates and stimulated with 25 μL/mL ImmunoCult Human CD3/CD28 T-Cell Activator (StemCell) on day 0. Cell density was adjusted to 1–2x10⁶ cells/mL with new culture medium containing 100 U/mL IL-2 every 2–3 days.

CIK cells were cultivated as previously described (46): In brief, cells were resuspended at a density of 3x10⁶ cells/mL in RPMI 1640 with GlutaMAX and 10% FBS in 6-well plates and primed by adding 1000 U/mL Interferon-γ (IFNγ, Boehringer Ingelheim) on day 0. 100 ng/mL anti-CD3 antibody (MACS GMP CD3 pure, Miltenyi Biotech) and 500 U/mL IL-2 were added after 24 h. 50 ng/mL human IL-15 (Peprotech) was added on day 3. Over the course of the culture, cell density was adjusted to 1x10⁶ cells/mL, fresh medium and 50 ng/mL IL-15 were added on day 5 and 8.

To generate ErbB2-CAR-CIK and CAR-T cells, transduction with lentiviral particles (produced using the pS-5.28z-IEW transfer plasmid) was performed via spinfection on day 2 of culture. The pS-5.28z-IEW vector was described previously (34, 44, 47): it encodes a codon-optimized second-generation CAR with the ErbB2-specific scFv (FRP5) antibody fragment, modified CD8α hinge region, CD28 transmembrane and intracellular domains and a CD3ζ intracellular domain inserted upstream of IRES and eGFP sequences of the pSIEW vector backbone (48). eGFP was used as a fluorescence marker. Transduction protocols were optimized to achieve comparable CAR-expression in CAR-CIK and CAR-T cells. For T cells, the cell number was adjusted to 0.25x10⁶ cells/well, 8 μg/mL polybrene (Sigma-Aldrich) and 100 μL viral particles were added and volume was topped up to 1 mL/well with culture medium. For CIK cells, the cell number was adjusted to 0.5x10⁶ cells/well, 8 μg/mL polybrene and 1000 μL viral particles were added and volume was topped up to 2 mL/well with culture medium. Spinfection was done at 800 g (acceleration 4/10, no brake) for 50 minutes at 32°C. Afterwards, half of the culture medium was exchanged with fresh culture medium containing IL-2 (100 U/mL) for transduced T cells, whereas transduced CIK cells were incubated for 24 hours and then stimulated with 50 ng/mL IL-15. T cell density was adjusted to 1–2x10⁶ cells/mL with new culture medium containing 100 U/mL IL-2 every second or third day. CIK cell density was adjusted to 1x10⁶ cells/mL at day 5 and 8 of culture and fresh culture medium and 50 ng/mL IL-15 were added. All cells were expanded over 10 days and then used for further analyses. Effector cell numbers utilized in experiments encompass the entire population without specific selection for CAR+ cells, ensuring representation of the heterogeneous CIK cell population, including NK and TNK cells transduced at a lower rate. Transduction methods were optimized to ensure equal CAR-expression rates in bulk CAR-CIK and CAR-T cells across all analyses.

2.4 Luciferase toxicity assay

RMS cells stably expressing firefly luciferase (fLuc) were used for 24 h toxicity assays as previously described (49). Effector cells were added at effector to target (E:T) ratios from 10:1 to 1.25:1. Results are given as percentage of luciferase signal of untreated target cells.

2.5 Spheroid co-incubation assay

For generation of Rh30fLuc/mCherry and Rh41fLuc/mCherry spheroids, 5×10^3 cells were seeded in 200 μ L of RPMI with 10% FBS into ultralow attachment 96-well round-bottom plates without prior coating (Corning). After 4 days, 100 μ L of supernatant was removed, and 25×10^3 , 12.5×10^3 or 6.25×10^3 effector cells resuspended in 100 μ L medium (without cytokines) were added. Spheroids without effector cells were used as controls. Experiments were set up in duplicates. Co-cultures were incubated at 37°C and imaged every 8 hours using the Incucyte S3 System (Incucyte 202B, Sartorius) for 6 days. Half of the medium was exchanged after 3 days (no additional cytokines). The spheroid feature of the Incucyte S3 software was used to quantify growth of mCherry+ spheroids by measuring the integrated red intensity over time. After co-incubation with Rh30fLuc/mCherry spheroids, effector cells were analyzed via flow cytometry.

2.6 Whole cell proteomics

For whole cell proteomics, CAR-CIK, CAR-T and untransduced parental cells were co-incubated \pm Rh30 cells at an E:T ratio of 2:1. After 24 hours, CD45+ effector cells were isolated via FACS (CD45 PacificBlue, HI30, Biolegend) using a BD FACS Aria 3, collected into 1.5 mL tubes (Eppendorf), spun down and cryopreserved. Sample preparation, fractionation and liquid chromatography mass spectrometry was performed as described in the [Supplementary Methods](#). As no relevant differences were observed for the condition \pm RMS, results were aggregated for each effector cell. For data analysis and plotting, R version 4.2.2 was used together with data.table 1.14.10 and ggplot2 3.4.4. Differential expression changes comparing CAR-CIK vs. CAR-T cells were analyzed using DEqMS 1.16.0. For KEGG pathway analysis, the list of all quantified proteins was ranked (absolute \log_2 fold change \times $-\log_{10}$ -transformed q-value) and gene set enrichment analysis was done with clusterProfiler version 4.6.2 using default settings and FDR-correction of P values. The mass spectrometry proteomics data have been deposited to the ProteomeXchange Consortium via the PRIDE partner repository (50) with the dataset identifier PXD050654.

2.7 *In vivo* metastatic RMS xenograft model

Female non-obese diabetic (NOD)/severe combined immunodeficient (SCID)/IL-2receptor γ $^{-/-}$ (NSG) mice were used (age 6–12 weeks). To mimic the clinical situation of residual RMS after heavy pretreatment (44), mice were sublethally irradiated with

2.5 Gy (Biobeam 2000) on day -1. One day later (d0), 1×10^5 Rh30GFP/fLuc+ cells resuspended in 100 μ L of PBS were injected via the tail vein, allowing for metastatic tumor spread into liver, lungs and bone marrow. Mice were randomly divided into five different groups: control animals (n=7) received 100 μ L medium (GlutaMAX with 10% FBS) and treatment groups (CAR-CIK, CAR-T, CIK, T) received 2.5×10^6 effector cells resuspended in 100 μ L medium via tail vein injection on day +1. Group sizes were predetermined based on prior data (n=10–12 mice for CAR-engineered cells; n=5–6 for parental cells; \geq 5 animals with vehicle control). Tumor growth was monitored weekly by bioluminescence imaging (BLI) using an IVIS Lumina II system (Perkin Elmer). Mice were anesthetized via isoflurane inhalation and 1500 μ g *in vivo* grade VivoGlo luciferin (Promega) in 100 μ L PBS was injected subcutaneously. After 15 min, images were acquired at serial exposure times (1 s–4 min) and analyzed with Aura Spectral Instruments imaging software version 2.7.11. Photon flux was quantified per mouse in uniform regions of interest.

Animal experiments were approved by the responsible government oversight committee (Regierungspräsidium Darmstadt, Dezernat V54, ref. FK/2033). All applicable guidelines for housing, care and use of animals were followed. Mice were inspected minimum once daily, assessed and scored for disease activity; moribund mice were sacrificed. Peripheral blood, bone marrow (BM), lung, liver and spleen samples were isolated and analyzed for persistence of human tumor or effector cells (49): In brief, organs were cut in half and partly conserved in formaldehyde for immunohistochemistry. The remaining organ tissue was processed into single cell suspensions and analyzed via flow cytometry for human CD45+ effector cells.

2.8 Supplementary methods

A detailed description of cell lines, flowcytometry staining and antibodies, the detection of immune effector molecules via bead-based immuno-assay, immunohistochemistry of mouse organs, histology of primary patient material as well as a more detailed description of lentiviral particle production, transduction of cell lines, luciferase-based toxicity assays, whole cell proteomics and animal experiment reporting can be found in the [Supplementary Material](#).

2.9 Statistics

For statistical analysis and plotting, GraphPadPrism 10.2.0, R 4.2.2, data.table 1.14.10, ggplot2 3.4.4 and DEqMS 1.16.0 were used. Unless otherwise indicated in the figure legends, data are displayed as arithmetic mean \pm standard error of the mean (SEM). The exact sample size for each experimental group or condition is given in the figure legends. Only biological replicates are shown and used for statistical inferences. Where applicable, paired t-tests were used, otherwise the statistical method is described in the figure legend. Survival analyses were performed using the Kaplan-Meier method and Log-rank (Mantel cox) tests to compare treatment-groups.

Group differences with $p < 0.05$ (*), $p < 0.01$ (**) or $p < 0.001$ (***) were considered statistically significant.

3 Results

3.1 ErbB2-CAR CIK cells are easily produced by lentiviral transduction and maintain their distinctive CIK cell phenotype of TNK cells

To enable direct comparison, CIK and T cells were derived in parallel from same-donor PBMCs with a minimum of three independent donors (Figure 1A). Lentiviral transduction on day 2 of culture resulted in robust and equal CAR-expression in both CAR-CIK and CAR-T cells (GFP+ in CAR-CIK $35.7\% \pm 1.7\%$ vs. $33.7\% \pm 2.2\%$ in CAR-T, not significant) (Figures 1B, C, Supplementary Figure 1). CAR-CIK cells developed a mixed double-positive TNK population, with $21.2\% (\pm 3.9\%)$ of cells expressing both CD3 and CD56. The TNK population was negligible among CAR-T cells (Figure 1D). Transduction was most efficient in the CD3+CD56- T cell and the CD3+CD56+ TNK cell subpopulation of CAR-CIK cells and was seen to some extent in the CD3-CD56+ NK cell compartment of CAR-CIK cells (Figure 1E). CAR-CIK cells showed a predominant CD8+ cytotoxic phenotype, whereas CAR-T cells showed a CD4+ helper T cell phenotype (Figures 1F, G). *In vitro* expansion led to a reduction in naïve cells among both effector cell populations and to a shift towards a central memory and effector memory phenotype, with a higher percentage of naïve cells seen among CAR-CIK compared to CAR-T cells (Figure 1H, Supplementary Figure 1). Both transduced cell populations displayed high viability and equal expansion over the course of 10 days in culture (Supplementary Figure 1). Thus, CAR-CIK and CAR-T cells can be generated easily by lentiviral transduction at equal transduction rates, with CAR-CIK cells developing the distinctive TNK and effector phenotype of CIK cells.

3.2 ErbB2-CAR CIK cells show superior *in vitro* cytotoxicity

In 2D *in vitro* co-cultures with RMS cell lines and primary patient material (Figure 2A), we observed potent anti-tumor activity of CAR-CIK and CAR-T cells in a dose-dependent manner. Against the alveolar RMS cell line Rh30, CAR-CIK cells proved more efficacious than CAR-T cells at all effector to target (E:T) ratios (Figure 2B). For the TP53-mutated alveolar RMS cell line Rh41, we observed a less pronounced yet equally potent cytotoxicity of CAR-CIK and CAR-T cells (Figure 2C). Next, we tested both CAR-effector cells against primary tumor samples (H1, H9) obtained from relapsed, metastatic pediatric RMS that were confirmed to express ErbB2 via flow cytometry (Supplementary Figure 2). We observed a clear trend towards superior cytotoxicity of CAR-CIK cells compared to CAR-T cells, as well as dose-dependent increased efficacy at higher E:T ratios (Figures 2D, E). Overall, a linear regression model across all target cell types and E:T

ratios confirmed significantly higher killing of CAR-CIK compared to CAR-T cells (Figure 2F).

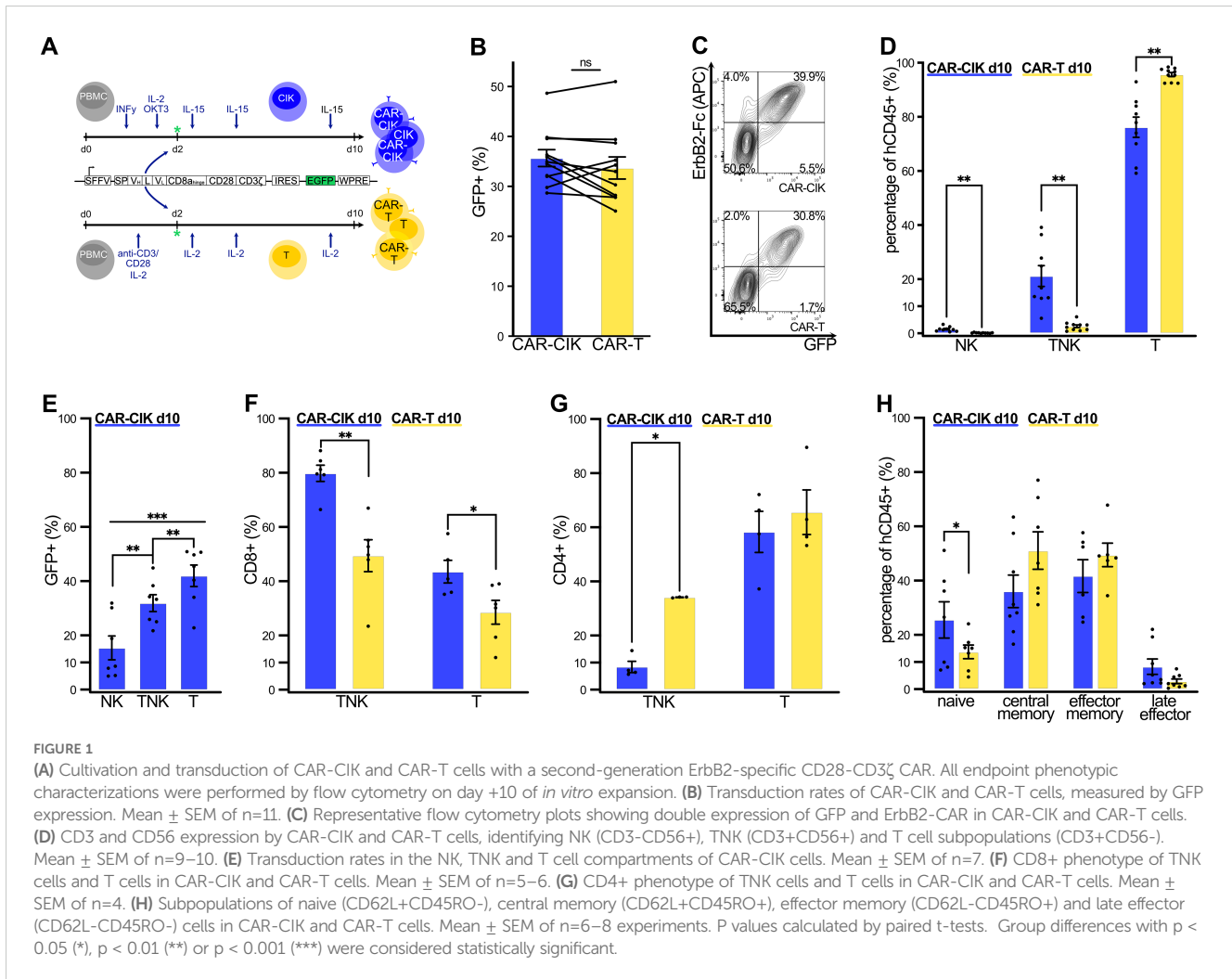
To further confirm the potency of CAR-CIK cells in 3D models, we generated RMS tumor spheroids and performed long-term co-cultivation of the CAR effector cells with established tumor spheroids (Figure 2G). Over the course of 6 days, both CAR-effector cells potently inhibited spheroid growth and even led to lysis of Rh30 tumor spheroids at higher concentrations, with CAR-CIK cells proving more potent than CAR-T cells at the highest E:T ratio (Figure 2H). Against Rh41 spheroids, CAR-CIK proved more efficacious than CAR-T cells at two out of three assessed effector concentrations (Figure 2I). Taken together, these results show superior killing activity of CAR-CIK vs. CAR-T cells in multiple *in vitro* models of RMS.

3.3 CAR-CIK cells proliferate and show enrichment of CAR+ and TNK cells upon target exposure

Analysis of effector cells after long term co-incubation with Rh30 tumor spheroids over 6 days without additional cytokine stimulation (Figure 3A) revealed that CAR-CIK cells proliferated upon target exposure, whereas CAR-T cells did not (Figure 3B). The GFP+ population (GFP being co-expressed with the CAR) was significantly enriched only in CAR-CIK cells after spheroid co-incubation, indicating preferential expansion of CAR-bearing CIK cells (Figure 3C). Furthermore, prolonged co-culture with RMS spheroids led to an increase of the CD3+CD56+ TNK cell compartment of CAR-CIK cells (Figure 3D). After co-culture, CAR-CIK cells showed a predominant CD8+ phenotype, while there was no significant change in the CD8+ phenotype of CAR-T cells (Figure 3E). Likewise, the memory/naïve phenotype of CAR-T cells did not change appreciably after co-culture (Figure 3F). By contrast, CAR-CIK cells displayed a considerable change, with fewer naïve cells and more effector memory cells. CAR-CIK cells co-incubated with RMS spheroids also contained a smaller population of central memory and a higher proportion of terminal effector cells than CAR-T cells (Figure 3F). These results show that CAR-CIK cells exhibit clear phenotypical changes upon RMS target contact with preferential expansion of CAR-bearing cells and acquisition of effector cell characteristics, unlike CAR-T cells.

3.4 CAR-CIK cells show NK cell cytotoxicity *in vitro*

We next sought to analyze modes of action of CAR-CIK and CAR-T cells (Figure 4A). After 24 h co-incubation with Rh30 cells, cytokine profiles in the supernatants of CAR-CIK and CAR-T cells differed profoundly. Whereas CAR-T showed high secretion of IL-2, IL-4 and IL-10, which had a very low concentration in CAR-CIK conditioned media, CAR-CIK supernatants contained high levels of effector cytokines and direct mediators of cytotoxicity, such as IFN γ , granzysin, perforin, granzymes and soluble Fas-Ligand (sFasL). IL-6 and TNF α were found at similar levels in both conditions (Figures 4B–L).



To identify potential differences in CAR-CIK and CAR-T cells responsible for these contrasting cytokine secretion profiles, we performed whole cell proteomics and measured differentially expressed proteins in CAR-CIK and CAR-T cells as well as untransduced parental CIK and T cells. Cells were FACS-purified and prepared for liquid chromatography mass-spectrometry using tandem-mass tag (TMT)-based multiplexing and offline fractionation. This approach quantified 7101 distinct proteins (Figure 4M). Unsupervised clustering showed excellent separation in protein expression according to cell type and transduction status (Figures 4N, O). Proteins significantly depleted in CAR-CIK cells compared to CAR-T cells were negative regulators of T cell activation (HOMER2, CTLA4), proteins expressed in Th2 cells (HPGDS, GPX1) and during CD4+ activation (LGMN) as well as proteins negatively influencing T cell function (ARG2, MAO-A). Proteins found to be significantly enriched in CAR-CIK cells pertained to NK cell differentiation (NCAM1/CD56), TNK cell differentiation (TRGC1), CD8 (CD8B, CD8A) and Th1 differentiation (ANXA3), INF γ response (TBX21, HBB), vesicle formation (STX3, ANXA3), granzyme B secretion (CTSH, TBX21), activated (NK) cells (ENTPD1, AFAP1L2) and cellular cytotoxicity of NK cells (CTSW, TBX21) (Figure 4P, Supplementary Table 1). Finally, unbiased KEGG pathway analysis of whole cell proteomics data revealed NK cell

mediated cytotoxicity, chemokine signaling, Rap1 signaling (mediating NKG2D-driven cytotoxicity) (51), NF- κ B signaling and Fc- γ receptor signaling as some of the most relevant pathways overexpressed in CAR-CIK cells compared to CAR-T cells (Figure 4Q). These profound mechanistic differences strongly suggest that CAR-CIK cells, despite their CD3+ T cell majority and the CAR-transduction, act like NK cells in conveying their cytotoxicity.

3.5 CAR-CIK effector cells demonstrate equal potency in an *in vivo* metastatic RMS xenograft model

We next wanted to compare the *in vivo* efficacy of the CAR-effector cells using a metastatic RMS xenograft model mimicking minimal residual disease. After sublethal irradiation, NSG mice received luciferase-expressing RMS tumor cells (Rh30GFP/fLuc) via tail vein injection. 24 h later, mice were randomized into five experimental groups and treated with (1) 2.5×10^6 CAR-CIK cells, (2) 2.5×10^6 CAR-T cells (with equal CAR-expression, Supplementary Figure 3B), (3) 2.5×10^6 parental CIK cells, (4) 2.5×10^6 parental T cells, or (5) vehicle control. Tumor burden

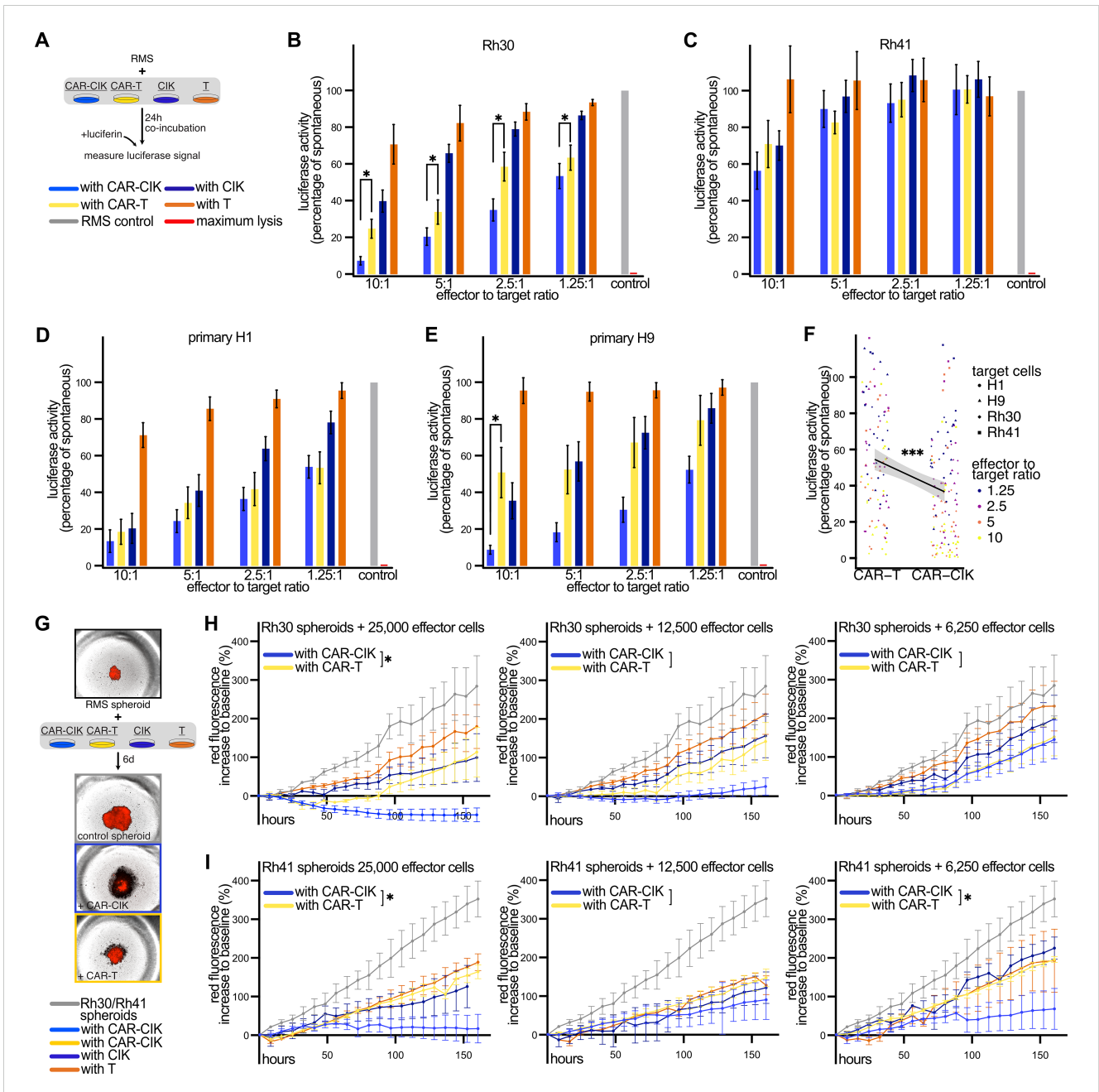


FIGURE 2

(A) Experimental scheme. Co-incubation of parental and ErbB2-CAR-CIK and CAR-T cells and T cells with luciferase-expressing target cells for 24 h at different effector to target ratios. Results are given as percentage of luciferase signal of untreated target cells served as maximum lysis control. (B–E) Cytotoxicity against B) Rh30 (n=8–10), (C) Rh41 (n=3–4), and against primary patient-derived tumor cells (D) H1 (n=6–9) and (E) H9 (n=6–7). Mean ± SEM are shown. P values calculated by Wilcoxon tests comparing CAR-CIK vs. CAR-T cells. (F) A linear regression model was used to compare the effect of CAR-CIK vs. CAR-T cells across all four target cells and all effector to target ratios with these parameters as independent predictors. Individual values and regression line with 95% confidence interval (shaded grey area) are shown. (G) Experimental scheme with representative microscopy images. (H, I) Parental and CAR effector cells were co-incubated for 6 d with established tumor spheroids generated from Rh30mCherry (H, n=5) or Rh41mCherry cells (I, n=3) and monitored via fluorescence microscopy. Difference to baseline (1 h after effector cell addition) of red fluorescence of the tumor spheroids is given in percent. Mean ± SEM are shown. P values by unpaired t-tests, comparing areas under the curves (AUC). Group differences with $p < 0.05$ (*), $p < 0.001$ (***) were considered statistically significant.

and disease progression were assessed by weekly bioluminescence imaging (BLI) and clinical scoring for a period of 100 days (Figure 5A). Every animal developed tumors detectable via BLI. CAR-CIK- and CAR-T-treated mice showed significantly lower BLI tumor burden than controls (Figures 5B, C). Tumor growth progressed most rapidly in vehicle control mice, with a median survival of 63 days (range, 39–66 days; Figure 5D). Neither

untransduced CIK nor T cells significantly slowed tumor growth in comparison to controls (CIK cells: median survival 60 days, range 45–84 days; T cells: median survival 66 days, range 49–72 days; Figure 5D). However, the single application of either CAR-CIK or CAR-T cells markedly delayed metastatic tumor development and significantly improved the duration of survival compared to parental immune effector cells or controls. CAR-T-treated

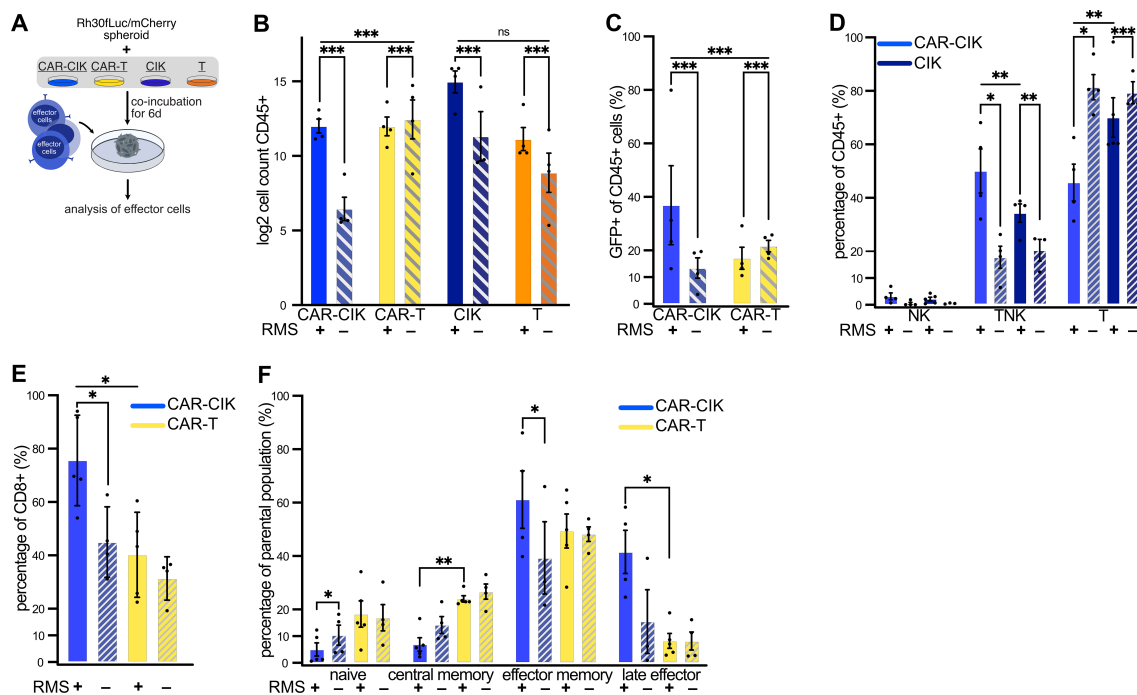


FIGURE 3

(A) Experimental scheme. Flow cytometric analysis of effector cells after 6 d co-incubation of parental and ErbB2-CAR-CIK and ErbB2-CAR-T cells with Rh30 spheroids. (B) Effector cell counts (log₂-transformed) after 6 d ± RMS spheroids. Mean ± SEM of n=3–4; comparison of ± RMS by Poisson regression on untransformed count data; between-group effect of ± RMS was compared between CAR-CIK and CAR-T by testing for differences in slope of Poisson regression lines (likelihood ratio test). (C) Percentage of GFP⁺ cells after 6 d ± RMS. Mean ± SEM of n=4; analysis by Poisson regression as done in (B, D) CD3 and CD56 expression of CAR-CIK and CIK cells after 6 d ± RMS given as percentages of NK cells (CD3⁺CD56⁺), TNK cells (CD3⁺CD56⁺) and T cells (CD3⁺CD56⁻). Mean ± SEM of n=3–5, comparing CAR-CIK + RMS vs. CIK + RMS, CAR-CIK + vs. – RMS and CIK + vs. – RMS. P values by paired t-tests. (E) Relative CD8 expression of CAR-CIK and CAR-T cells after 6 d ± RMS. (F) Relative sizes of naive (CD62L⁺CD45RO⁻), central memory (CD62L⁺CD45RO⁺), effector memory (CD62L⁻CD45RO⁺) and terminal effector (CD62L⁻CD45RO⁻) subpopulations after 6 d ± RMS of CAR-CIK and CAR-T cells. Mean ± SEM of n=3–4 (E) and n=3–5 (F). P values by paired t-tests, comparing CAR-CIK + RMS vs. CAR-T + RMS, CAR-CIK + vs. – RMS and CAR-T + vs. – RMS, respectively. Group differences with p < 0.05 (*), p < 0.01 (**) or p < 0.001 (***) were considered statistically significant.

animals showed a median survival of 86 days (range 58–100 days), while CAR-CIK-treated animals showed a median survival of 97 days (range 65–100 days). Thus, the metastatic RMS model showed equipotency of CAR-CIK cells *in vivo*.

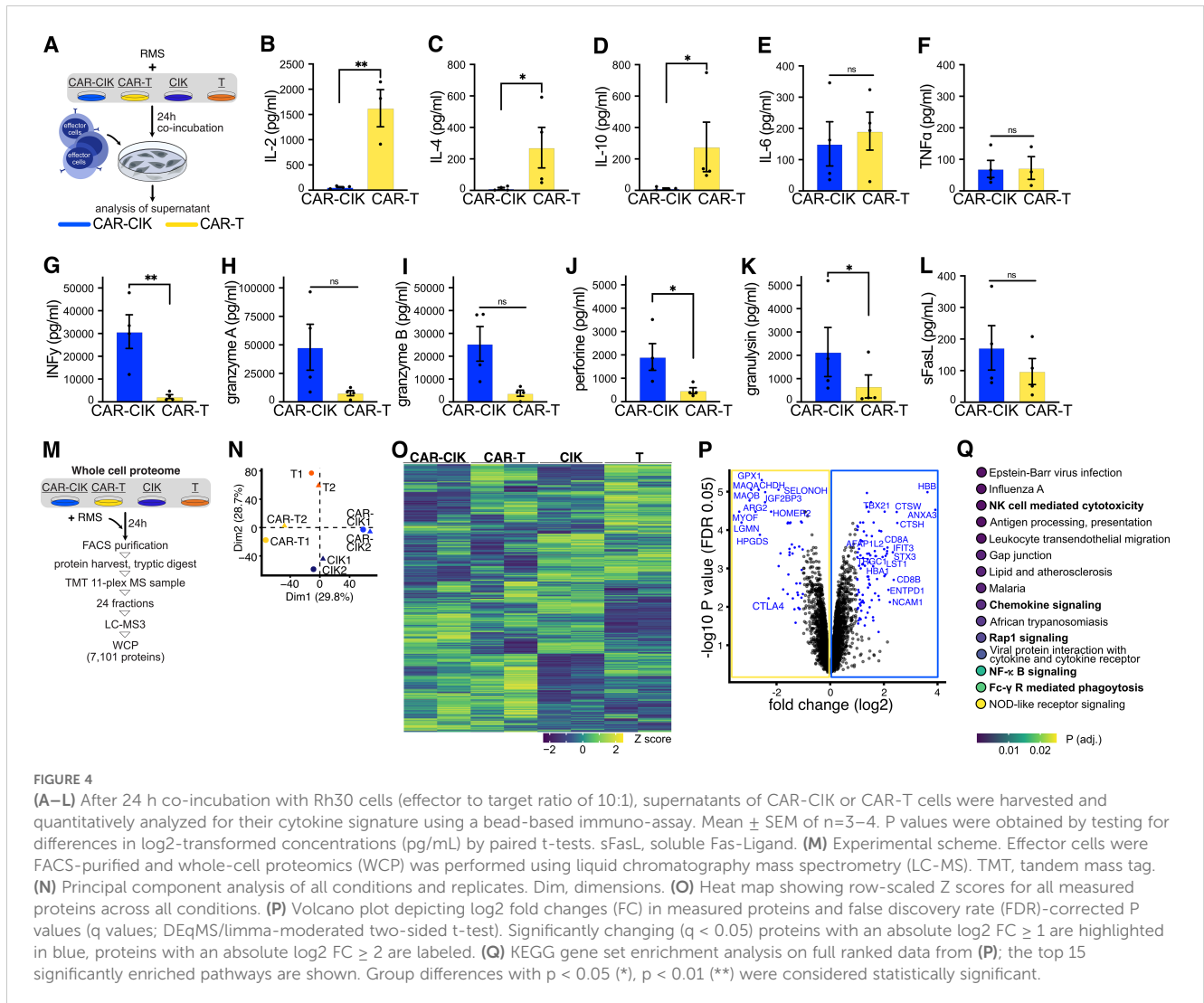
3.6 ErbB2-CAR-CIK cells migrate to tumor-infiltrated organs and display a predominant effector phenotype *in vivo*

Blood, bone marrow (BM), spleen, liver and lungs were collected from each animal at the time of death to assess persistence and distribution of effector cells. Human CD45⁺ (hCD45⁺) cells were detectable via flow cytometry in all assessed organs of 6/10 CAR-CIK-treated animals (not being detected in any organ in 2/10 animals and detected in BM and lungs of n=1 and only in the blood of n=1; Figure 6A, Supplementary Figure 3). In contrast, only 2/12 CAR-T-treated animals had detectable hCD45⁺ cells in all assessed organs (not detected in any organ in 2/12 animals and detected in multiple but not all organs in 8/12; Figure 6A, Supplementary Figure 3). Among hCD45⁺ cells, we observed equal proportions of GFP⁺ CAR-bearing cells among CAR-CIK- and CAR-T-treated animals (Figure 6B). In blood, BM,

spleen and liver samples, the majority of analyzed cells from CAR-CIK-treated animals were CD8⁺, whereas cells from CAR-T-treated animals were mostly CD8⁻ (Figures 6C, D). CAR-CIK and CIK cells retrieved from the assessed organs retained their composition of a mixed TNK cell phenotype (Figures 6E, F), whereas CAR-T cells had a sole CD3⁺ T cell phenotype (Supplementary Figure 3D). In all analyzed organs from animals treated with both CAR-CIK and CAR-T cells, the majority of retrieved cells exhibited an effector memory phenotype, with smaller populations of central memory and late effector cells (Figure 6G). Finally, immunohistochemistry analysis for hCD45⁺ cells in representative organ samples confirmed migration of both CAR-effector cells to lungs, livers and spleens (Figure 6H). Despite the constraints of these endpoint analyses, these findings show that CD8⁺ effector phenotype CAR-CIK cells migrated to multiple organs affected by metastatic RMS and indicate effector cell persistence for an extended period *in vivo*.

4 Discussion

The advance of CAR technology has revolutionized the treatment of certain hematological malignancies, achieving very promising results, both in a clinical-trial context and in the real-

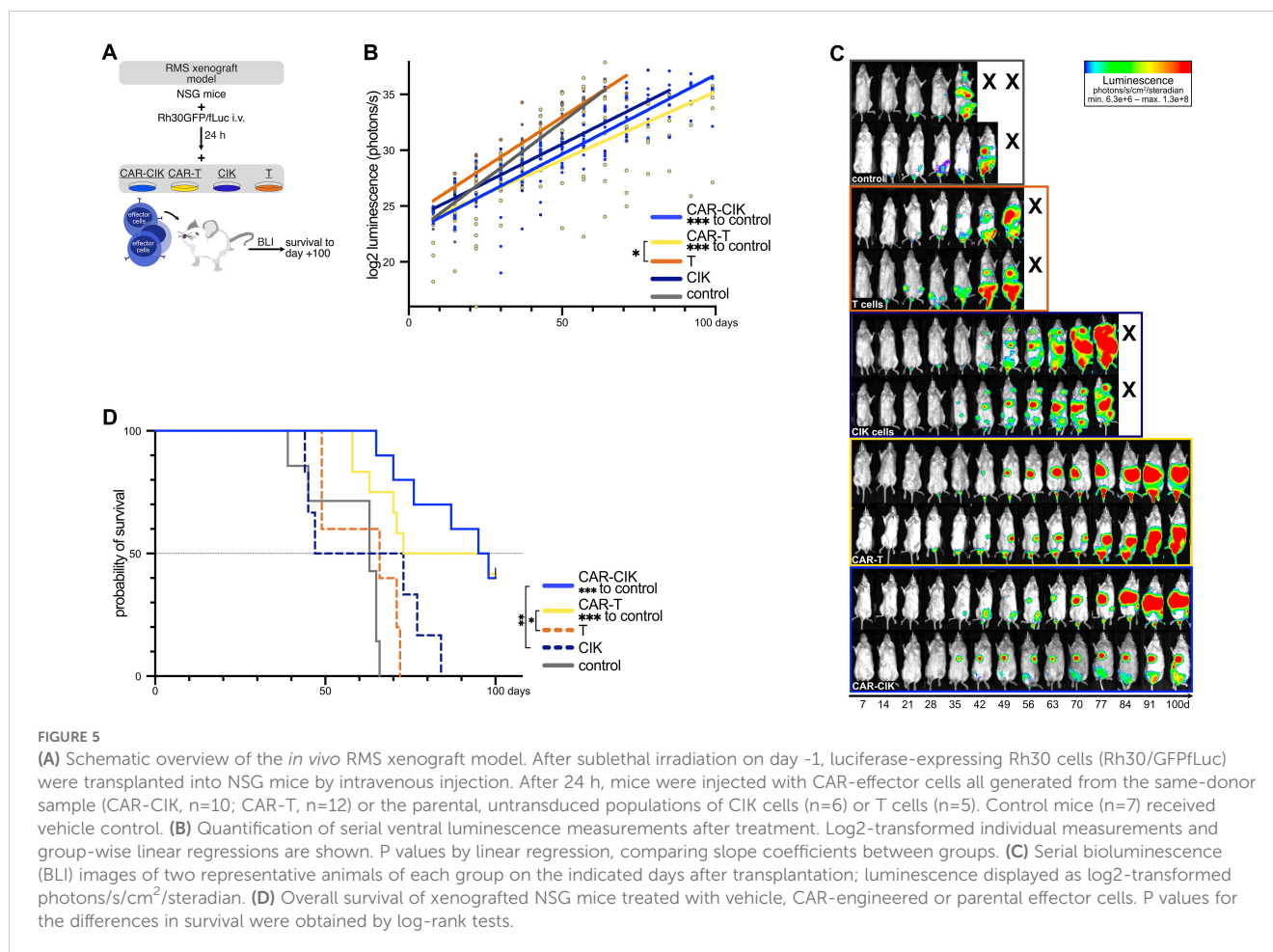


world (1–5). However, the success of CAR-T cell therapy is still limited for solid tumors (6, 7). Several factors impede CAR-T cell applications, such as insufficient homing into the tumor-afflicted organs, tumor heterogeneity, antigen escape and the hypoxic and immunosuppressive environment in bulk tumors. Tumor-associated regulatory T cells and macrophages, as well as ligands for checkpoint receptors expressed by the tumor cells suppress effector cell function *in situ* (7–9). Further, heavy pretreatment of metastatic tumor patients compromises the number and quality of autologous T cells, leading to dysfunction, exhaustion and poor persistence (6, 10).

One strategy to improve adoptive cellular therapy in solid cancer is the use of healthy donor cells for CAR-engineering (9, 10, 12, 13). Allogeneic T cells cannot be used as effector cells outside the setting of allo-HSCT due to potentially lethal GvHD without additional genetic modifications that add complexity to the manufacturing process and introduce new safety concerns (10, 12). By contrast, CIK cells are a population of potent effector cells that can be safely employed across allogeneic barriers (16–20). We and others have previously shown that RMS can be successfully targeted using ErbB2-specific CAR-CIK cells (34, 41, 43, 44). We

chose RMS as a model to benchmark CAR-CIK cells against conventional CAR-T cells because there is a high clinical need to develop new treatment strategies for pediatric metastatic RMS (39). To our knowledge, this is the first study to directly compare the efficacy and mode of action of these two immune effectors generated from same-donor samples (52).

To facilitate clinical translation, we utilized a second-generation CD28-CD3 ζ CAR previously shown to mediate ErbB2-specific effects (34, 47, 53). A very similar CD28-CD3 ζ CAR harboring the same FRP5-derived single-chain fragment variable antibody domain has been safely employed in phase I/II CAR-T clinical trials in pediatric patients with ErbB2+ sarcoma (41–43). In our study, both T and CIK cells from several independent donors could easily be transduced with lentiviral vector particles and displayed robust CAR expression. We confirmed that the typical CD3+CD56+ TNK cell phenotype of CIK cells also develops after lentiviral transduction (34, 44). By optimizing transduction methods, we ensured equal CAR-expression among the bulk populations of CAR-CIK and CAR-T cells used in all experiments. CAR-CIK cells consistently showed more effective killing of RMS cell lines and primary patient tumor cells in 2D culture and inhibited tumor

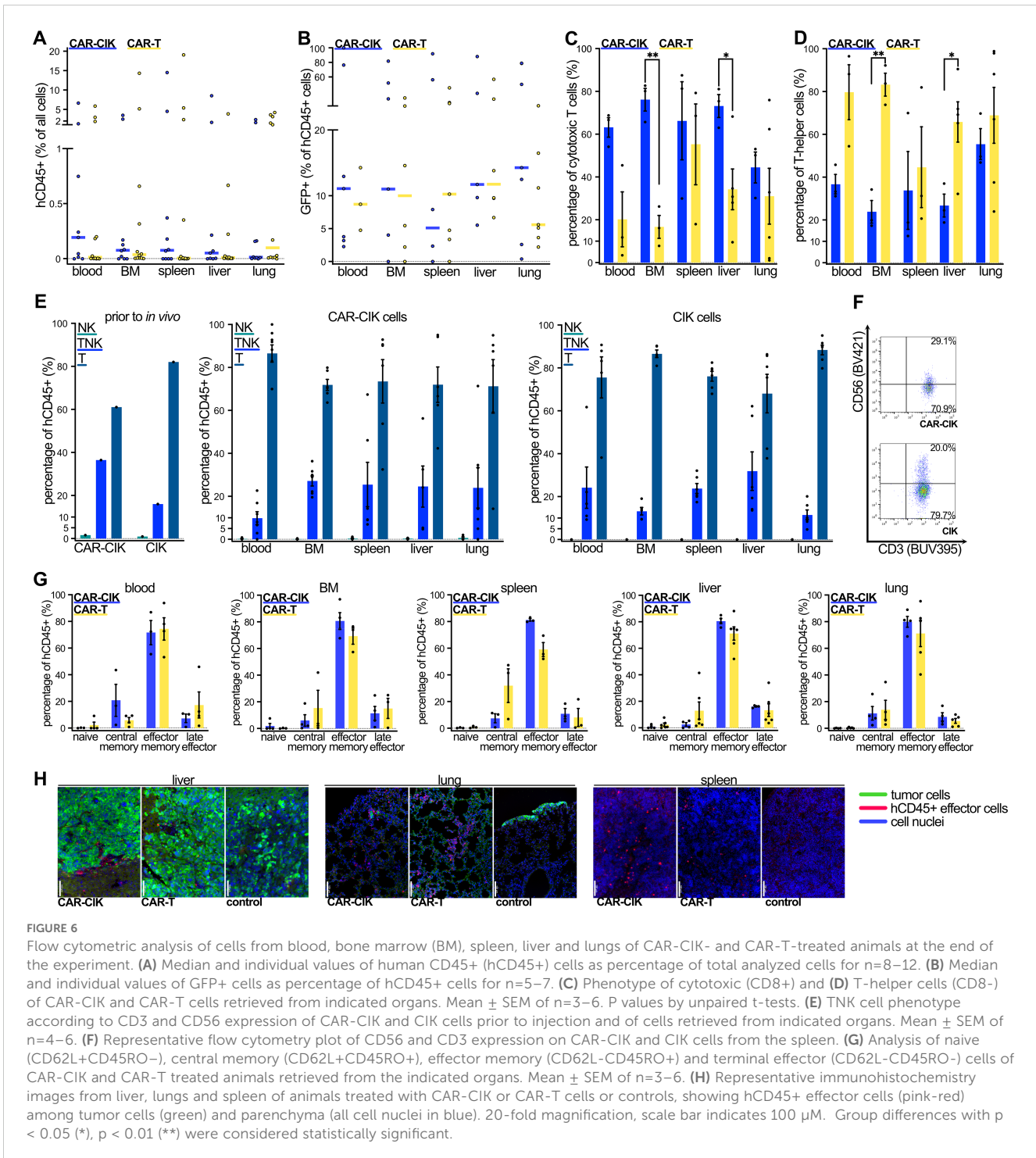


spheroid growth more potently than CAR-T cells, albeit not statistically significant across all E:T ratios. Importantly, only CAR-CIK cells expanded and changed their phenotype upon RMS tumor target exposure. Despite being a predominant T cell population, CAR-CIK cells apparently conveyed their cytotoxicity via NK cell mechanisms of action. These results underline that both effector cell populations differ not only in their phenotype, but also with regard to their functionality. Finally, a xenograft model of metastatic RMS showed equal potency and improved persistence of CAR-CIK cells *in vivo*.

CIK cells have a much lower allo-reactive potential than T cells and maintain their low allo-reactivity after CAR-engineering (16–20). They can be safely applied to patients at dosages more than ten times exceeding the usual T-cell dosage for donor lymphocyte infusions in a haploidentical setting after HSCT (refs (20, 54). and unpublished results of the FFM-CIK-Cell Study 01, Eudra-CT: 2013-005446-11). Allogeneic CIK cells have been approved in Germany as an advanced therapy medicinal product (ATMP) for children and adults with impending relapse of hematologic malignancies after allo-HSCT (ATMP §4b Abs. 3 AMG, license number: PE.LA.11630.01.1) (55). In pediatric RMS patients, one envisioned avenue of translation would be to use matched sibling or parent donors to ensure ample and healthy starting material and reduce any residual allo-reactive potential. Unlike CAR-T cells, allogeneic CAR-CIK cells can be used without additional genetic engineering of the original T cell receptor,

thus improving *in vivo* persistence (56) and avoiding additional costs and potential genotoxicity (10, 12).

In the clinic, cytokine-release syndrome (CRS) and neurotoxicity represent the most relevant and potentially life-threatening side effects of CAR-T cell therapy (57). Their pathophysiology has not been fully understood and it is difficult to predict outcomes based on immunodeficient *in vivo* models (57). However, all clinical studies involving CIK and CAR-CIK cells have consistently shown excellent safety profiles (15, 21). Furthermore, encouraging complete response rates without any GvHD or neurotoxicity (and only grade 1–2 CRS) were recently reported in relapsed B-ALL patients after allo-HSCT using donor-derived anti-CD19-CAR-CIK cells (NCT03389035) (18). In our own analyses, CAR-CIK cell cytokine signature showed significantly higher levels of effector molecules such as INF γ , perforin and granulysin. By contrast, CAR-T cells showed high levels of IL-2 and IL-10 which have been linked to CRS (57) and also exhibited increased levels of cytokines linked to immunosuppression, such as IL-4 and IL-10 (58). In our phenotypical characterizations, we showed that CAR-CIK cells have a TNK cell phenotype and whole cell proteomics further indicated that their cytotoxicity is mediated via NK cell mode of actions. When used as adoptive cellular therapies, NK cells have so far not shown side effects of CAR-T cell therapy and demonstrated a favorable safety profile (59). Although a direct clinical safety evaluation is beyond the scope of this work, these



results, together with the established safety record of CIK and NK cell therapies, support the clinical advancement of CAR-CIK cells.

Using CIK cells as effector cells for CAR-engineering allows to combine CAR-mediated target specificity of synthetic biology with the potency of innate effectors. Loss of target antigen and antigen heterogeneity have emerged as major obstacles to single-target CAR-immunotherapy (6, 8, 9). As a heterogeneous population, CIK cells can recognize and target tumor cells in an HLA-dependent as well as an HLA-independent manner (15, 36, 37). We have previously shown that ErbB2-CAR-CIK cells convey

potent cytotoxicity against various RMS cell lines *in vitro* while retaining NKG2D-mediated cytotoxicity against ErbB2-negative tumors (34). Furthermore, CAR-mediated activation of CAR-CIK cells can improve their HLA-independent recognition of target cells (52) and support the adoptive immune system as well as bystander cells within the TME (44). Previous studies have shown that the cytotoxicity of (CAR-)CIK cells is conveyed by their mixed heterogeneous population (35) and multiple clinical trials have established the use of CIK cells as composite effector cells (21). We therefore used the bulk population of effector cells for

comparative analyses, encompassing CAR-transduced cells as well as NK and TNK cells, in which viral transduction rates were lower.

Elevated secretion of INF γ seems to be a key feature in CAR-CIK cell mediated cytotoxicity. It is not only important in promoting their reduced GvHD-potential (16), but also required for CAR-cell-mediated killing in solid tumors (60). INF γ signaling facilitates invasion of CAR-cells into tumor islets (61) and may promote the upregulation of MHC molecules on tumor targets and thereby enhance HLA-dependent toxicity (62). INF γ also activates macrophages and antigen-presenting cells, which can recruit and enhance the endogenous antitumor immune responses in an immunocompetent host (63). Although there is evidence for the role of INF γ in creating an immunosuppressive TME (63), we observed no increase in regulatory T cells among CAR-CIK cells and measured decreased expression of the immune checkpoint receptor/exhaustion marker PD-1 on CAR-CIK cells despite similar activation and expansion of both CAR-CIK and CAR-T cells after *in vitro* culture (as indicated by their CD69 expression; [Supplementary Figure 1](#)). We observed that CD39 was preferentially expressed in CAR-CIK cells, a molecule known to modulate immune responses through adenosine production (64). While CD39 is associated with exhaustion in T cells (64–66), its role in NK cells and the heterogeneous TNK population of CAR-CIK cells remains inconclusive (67–69). Emerging evidence suggests that CD39 in NK cells may support activation and is linked to IL-15 stimulation (68). Importantly, the only other significantly differentially expressed marker commonly linked to exhaustion in our analysis was CTLA4 (70), which was increased in CAR-T cells. Based on these findings and our flow cytometric analyses, we cannot claim that either CAR-CIK or CAR-T cells are more prone to exhaustion. Further investigation into the mechanisms of exhaustion and persistence in these effector cells would provide important insights and represents a promising direction for future research.

The efficacy of CAR-immunotherapy is highly dependent upon prior reduction of tumor load (4) and especially in the context of solid tumors CAR-effector cells will most likely not induce a remission in bulky disease (6). Hence, we used an established *in vivo* model with minimal residual tumor burden at the time of CAR cell infusion (35, 44, 46, 49), which develops into metastasized RMS if left untreated and is similar to other sarcoma mouse models used for immunotherapy (71, 72). Both CAR-effector cells mediated strong inhibition of tumor growth. The *in vivo* trafficking and biodistribution of CAR-CIK and CAR-T cells was analyzed by flow cytometry as well as IHC. Although the predominant effector memory phenotype of CIK cells has previously been associated with reduced persistence (27), we observed effector cells in all assessed organs of the majority of CAR-CIK-treated animals, compared to only a minority of CAR-T-treated animals, up to 100 days after a single injection. This may indicate sustained functionality and vitality of CAR-CIK cells and their ability to maintain efficacy over an extended period *in vivo*. Further analyses of these effector cells retrieved from target organs at multiple pre-planned time points after injection, including detailed phenotypic characterization and assessment of their *ex vivo* functionality, would provide valuable insights into differences in their modes of action and failure. Additionally, investigating the role of exhaustion in these effector cells would be highly informative and could elucidate mechanisms underlying their long-term *in vivo* persistence and

efficacy. Clinically, we see a role for CAR-immunotherapy in RMS not against bulky disease, but as a sequenced treatment to control residual disease after surgery and intensive chemo- and radiotherapy. As demonstrated in the clinical HER2-CAR-T trial by Hegde et al. repeated infusions of CAR-effector cells are probably necessary to achieve long lasting remission (43).

The conclusions of our work are limited to the conditions that we have analyzed. Although we have made use of multiple donors and different target cells, including primary patient material, we have only employed one CAR-design and cannot currently generalize beyond rhabdomyosarcoma. We have primarily focused our analyses on the efficacy of these effector cells, their cytokine responses, and the distinct phenotypic and functional properties associated with their mixed T cell and NK cell characteristics. While an in-depth comparison of factors linked to exhaustion and persistence would be highly valuable, it was beyond the scope of the current study. Furthermore, it is necessary to acknowledge the limitations of an immunodeficient mouse model, particularly regarding the absence of the original tumor microenvironment observed in patients and lack of additional immunosuppressive cells (73). However, immunodeficient mouse models are commonly used to assess efficacy (6, 71, 72) and this model allowed us to utilize the established ErbB2-specific CD28-CD3 ζ CAR (34, 47, 53) and human effector cells to facilitate clinical translation.

Taken together, this first comparison of CAR-CIK vs. CAR-T cells in solid tumors demonstrates that ErbB2-CAR cells generated from CIK cells can be robustly produced by lentiviral transduction and have more potent *in vitro* activity and equally strong *in vivo* potency as CAR-T cells. CAR-CIK cells exhibit phenotypic differences and distinct modes of actions characterized by a CD3+CD56+ TNK and effector phenotype and rely on NK cell modes of action, while demonstrating enhanced persistence compared to adoptively transferred NK cells (74). Due to their intrinsically varied endogenous antigen-specific and non-antigen-specific anti-tumor potency, they can provide additional benefits to the CAR. Importantly, their use as healthy donor cells in an allogeneic setting is feasible and safe without additional multi-level genetic engineering. These findings support the development of CAR-CIK cells as allogeneic immune effectors to advance cellular therapies in metastatic RMS and other solid tumors.

Data availability statement

MS-data are available on the public open-access repository PRIDE (<https://www.ebi.ac.uk/pride/>; dataset identifier PXD050654). Please direct any inquiries or requests for further raw data or additional information to the corresponding authors.

Ethics statement

The studies involving humans were approved by ethics review board of the Medical Faculty of the Goethe University (Frankfurt, Germany, RMS samples: SPO-04-2015, healthy donor PBMCs: Nr. 413/15). The studies were conducted in accordance with the local legislation and institutional requirements. Written informed consent for participation in this study was provided by the

participants' legal guardians/next of kin. The animal study was approved by Regierungspräsidium Darmstadt, Dezernat V54, ref. FK/2033. The study was conducted in accordance with the local legislation and institutional requirements.

Author contributions

LM: Conceptualization, Data curation, Formal Analysis, Funding acquisition, Investigation, Methodology, Project administration, Resources, Software, Validation, Visualization, Writing – original draft, Writing – review & editing. CH: Investigation, Methodology, Writing – review & editing. SK: Conceptualization, Data curation, Formal Analysis, Investigation, Methodology, Writing – review & editing. PW: Investigation, Methodology, Writing – review & editing. SB: Formal Analysis, Writing – review & editing. SH: Investigation, Writing – review & editing. HK: Validation, Writing – review & editing. MM: Conceptualization, Methodology, Writing – review & editing. CM: Formal Analysis, Resources, Software, Writing – review & editing. EG: Investigation, Resources, Writing – review & editing. MV: Investigation, Resources, Writing – review & editing. EU: Resources, Software, Writing – review & editing. HB: Conceptualization, Resources, Software, Writing – review & editing. J-HK: Resources, Software, Writing – review & editing. PB: Conceptualization, Funding acquisition, Resources, Software, Supervision, Writing – review & editing. WW: Conceptualization, Resources, Writing – review & editing. ER: Conceptualization, Funding acquisition, Project administration, Resources, Supervision, Writing – review & editing.

Funding

The author(s) declare that financial support was received for the research, authorship, and/or publication of this article. This work was supported by the Else Kröner Research Foundation (LM), by the LOEWE Frankfurt Cancer Institute (LM; ER; EU; HMWK III L 5-519/03/03.001-0015 to WW), by the Mildred-Scheel-Nachwuchszentrum (SEK; 70113301 to ER), by grants from the Parents' Association Help for Children with Cancer e.V. as part of the C3OMBAT consortium (ER, EU, PB, J-HK), by the German Cancer Aid (Stiftung Deutsche Krebshilfe, to EU; WW; PB), by Menschen für Kinder e.V. (EU; PW) and by the Deutsche Kinderkrebsstiftung (DKS A2023_01 to MV). The LC-MS system (easy nLC1200, Orbitrap Fusion LUMOS) used in this study was funded by the Deutsche Forschungsgemeinschaft (German Research Foundation, DFG; FuG project ID 403765277 to CM).

Acknowledgments

We thank Katja Stein for expert technical assistance with *in vivo* bioluminescence measurements and members of the Quantitative Proteomics Unit at IBC2 (Goethe University, Frankfurt), in particular Georg Tascher for support and expertise in proteomics

methodology and data analysis, Martin Adrian-Allgood for technical help and measurements and Kristina Wagner for preparing LC columns. We thank the staff of the Georg-Speyer-Haus animal facility for their exemplary care of the mice and the staff of the UCT biobank for their help with primary patient material. We also thank all volunteer donors and patients and their families who consented to providing primary material, as well as all members of the Department of Pediatrics, University Hospital Frankfurt, who participated in the treatment of RMS patients.

Conflict of interest

HB reports no conflicts of interest COI pertinent to the work at hand, but acknowledges research support from Bayer, Chugai, Erydel, Miltenyi, Polyphor, Sandoz-Hexal a Novartis company, Stage a Celgene company, Terumo BCT, and Unique; honoraria and speaker fees from Chugai, Fresenius, Genzyme, Kiadis, Medac, Miltenyi, Novartis, Sandoz-Hexal, and Terumo BCT; consultancy and membership in advisory boards for Apriligen, Boehringer-Ingelheim, Celgene a BMS company, Genzyme, Medac, NMDP, Novartis, Sandoz-Hexal, Stage, and Terumo BCT; royalties from Medac and stock ownership in Healthineers. J-HK declares to have no COI with regard to this manuscript, but acknowledges advisory roles for Bluebird Bio, Novartis, Roche and Jazz Pharmaceuticals. PB declares to have no COI with regard to the work at hand, but declares research grants from Neovii, Riemser, Medac, and BMS to institution; is a member of advisory boards for Novartis, Celgene, Amgen, Medac, Servier personal and institutional; has received speaker fees from Miltenyi, Jazz, Riemser, Novartis, and Amgen to institution; and declares a patent with and royalties from Medac. WW is named as an inventor on patents owned by Georg-Speyer-Haus that relate to ErbB2/HER2-specific CARs.

The remaining authors declare that the research was conducted in the absence of any commercial or financial relationships that could be construed as a potential conflict of interest.

The author(s) declared that they were an editorial board member of *Frontiers*, at the time of submission. This had no impact on the peer review process and the final decision.

Publisher's note

All claims expressed in this article are solely those of the authors and do not necessarily represent those of their affiliated organizations, or those of the publisher, the editors and the reviewers. Any product that may be evaluated in this article, or claim that may be made by its manufacturer, is not guaranteed or endorsed by the publisher.

Supplementary material

The Supplementary Material for this article can be found online at <https://www.frontiersin.org/articles/10.3389/fimmu.2025.1485817/full#supplementary-material>

References

- Maude SL, Frey N, Shaw PA, Aplenc R, Barrett DM, Bunin NJ, et al. Chimeric antigen receptor T cells for sustained remissions in leukemia. *N Engl J Med.* (2014) 371:1507–17. doi: 10.1056/NEJMoa1407222
- Gardner RA, Shah NN. CAR T-cells for cure in pediatric B-ALL. *J Clin Oncol.* (2023) 41:1646–8. doi: 10.1200/JCO.22.02345
- Myers RM, Jacoby E, Pulsipher MA, Pasquini MC, Grupp SA, Shah NN, et al. INSPIRED Symposium Part 1: Clinical Variables Associated with Improved Outcomes for Children and Young Adults treated with Chimeric Antigen Receptor T cells for B cell Acute Lymphoblastic Leukemia. *Transplant Cell Ther.* (2023) 29:598–607. doi: 10.1016/j.jct.2023.07.016
- Cappell KM, Kochenderfer JN. Long-term outcomes following CAR T cell therapy: what we know so far. *Nat Rev Clin Oncol.* (2023) 20:359–71. doi: 10.1038/s41571-023-00754-1
- Maude SL, Laetsch TW, Buechner J, Rives S, Boyer M, Bittencourt H, et al. Tisagenlecleucel in children and young adults with B-cell lymphoblastic leukemia. *N Engl J Med.* (2018) 378:439–48. doi: 10.1056/NEJMoa1709866
- Albelda SM. CAR T cell therapy for patients with solid tumours: key lessons to learn and unlearn. *Nat Rev Clin Oncol.* (2024) 21:47–66. doi: 10.1038/s41571-023-00832-4
- Hou AJ, Chen LC, Chen YY. Navigating CAR-T cells through the solid-tumour microenvironment. *Nat Rev Drug Discov.* (2021) 20:531–50. doi: 10.1038/s41573-021-00189-2
- Rafiq S, Hackett CS, Brentjens RJ. Engineering strategies to overcome the current roadblocks in CAR T cell therapy. *Nat Rev Clin Oncol.* (2020) 17:147–67. doi: 10.1038/s41571-019-0297-y
- Labanieh L, Mackall CL. CAR immune cells: design principles, resistance and the next generation. *Nature.* (2023) 614:635–48. doi: 10.1038/s41586-023-05707-3
- Depil S, Duchateau P, Grupp SA, Mufti G, Poirot L. Off-the-shelf allogeneic CAR T cells: development and challenges. *Nat Rev Drug Discov.* (2020) 19:185–99. doi: 10.1038/s41573-019-0051-2
- Elavia N, Panch SR, McManus A, Bikkanji T, Szymanski J, Highfill SL, et al. Effects of starting cellular material composition on chimeric antigen receptor T-cell expansion and characteristics. *Transfusion (Paris).* (2019) 59:1755–64. doi: 10.1111/trf.15287
- Themeli M, Riviere I, Sadelain M. New cell sources for T cell engineering and adoptive immunotherapy. *Cell Stem Cell.* (2015) 16:357–66. doi: 10.1016/j.stem.2015.03.011
- Hossain AKMN, Hackett CS, Brentjens RJ, Rafiq S. Multipurposing CARs: Same engine, different vehicles. *Mol Ther.* (2022) 30:1381–95. doi: 10.1016/j.ymthe.2022.02.012
- Wu X, Schmidt-Wolf IGH. An alternative source for allogeneic CAR T cells with a high safety profile. *Front Immunol.* (2022) 13:1–4. doi: 10.3389/fimmu.2022.913123
- Zhang Y, Schmidt-Wolf IGH. Ten-year update of the international registry on cytokine-induced killer cells in cancer immunotherapy. *J Cell Physiol.* (2020) 235:9291–303. doi: 10.1002/jcp.v235.12
- Baker J, Verneris MR, Ito M, Shizuru JA, Negrin RS. Expansion of cytolytic CD8 + natural killer T cells with limited capacity for graft-versus-host disease induction due to interferon γ production. *Blood.* (2001) 97:2923–31. doi: 10.1182/blood.V97.10.2923
- Nishimura R, Baker J, Beilhack A, Zeiser R, Olson JA, Segal EI, et al. *In vivo* trafficking and survival of cytokine-induced killer cells resulting in minimal GVHD with retention of antitumor activity. *Blood.* (2008) 112:2563–74. doi: 10.1182/blood-2007-06-092817
- Magnani CF, Gaipa G, Lussana F, Belotti D, Gritti G, Napolitano S, et al. Sleeping Beauty-engineered CAR T cells achieve antileukemic activity without severe toxicities. *J Clin Invest.* (2020) 130:6021–33. doi: 10.1172/JCI138473
- Oelsner S, Wagner J, Friede ME, Pfirrmann V, Genßler S, Rettinger E, et al. Chimeric antigen receptor-engineered cytokine-induced killer cells overcome treatment resistance of pre-B-cell acute lymphoblastic leukemia and enhance survival. *Int J Cancer.* (2016) 139:1799–809. doi: 10.1002/ijc.v139.8
- Merker M, Salzmann-Manrique E, Katzki V, Huenecke S, Bremm M, Bakhtiar S, et al. Clearance of hematologic Malignancies by allogeneic cytokine-induced killer cell or donor lymphocyte infusions. *Biol Blood Marrow Transplant.* (2019) 25:1281–92. doi: 10.1016/j.bbmt.2019.03.004
- Sharma A, Ren X, Rosato A, Sangiolo D, Wang Z, Tettamanti S, et al. Cytokine-induced killer (CIK) cells, successes and challenges: report on the first international conference dedicated to the clinical translation of this unique adoptive cell immunotherapy. *Cancer Immunol Immunother.* (2024) 73:21. doi: 10.1007/s00262-023-03605-1
- Bendelac A, Lantz O, Quimby ME, Yewdell JW, Bennink JR, Brutkiewicz RR. CD1 recognition by mouse NK1 + T lymphocytes. *Science.* (1995) 268:863–5. doi: 10.1126/science.7538697
- Bendelac A, Rivera MN, Park SH, Roark JH. Mouse CD1-specific NK1 T cells: development, specificity, and function. *Annu Rev Immunol.* (1997) 15:535–62. doi: 10.1146/annurev.immunol.15.1.535
- Imai K, Kanno M, Kimoto H, Shigemoto K, Yamamoto S, Taniguchi M. Sequence and expression of transcripts of the T-cell antigen receptor alpha-chain gene in a functional, antigen-specific suppressor-T-cell hybridoma. *Proc Natl Acad Sci U S A.* (1986) 83:8708–12. doi: 10.1073/pnas.83.22.8708
- Shin S, El-Diwayn R, Schaffert S, Adams EJ, Garcia KC, Pereira P, et al. Antigen recognition determinants of $\gamma\delta$ T cell receptors. *Science.* (2005) 308:252–5. doi: 10.1126/science.1106480
- Nörenberg J, Jaksó P, Barakonyi A. Gamma/delta T cells in the course of healthy human pregnancy: cytotoxic potential and the tendency of CD8 expression make CD56 + $\gamma\delta$ T cells a unique lymphocyte subset. *Front Immunol.* (2021) 11:596489. doi: 10.3389/fimmu.2020.596489
- Franceschetti M, Pievani A, Borleri G, Vago L, Fleischhauer K, Golay J, et al. Cytokine-induced killer cells are terminally differentiated activated CD8 cytotoxic T-EMRA lymphocytes. *Exp Hematol.* (2009) 37:616–28. doi: 10.1016/j.exphem.2009.01.010
- Gütgemann S, Frank S, Strehl J, Schmidt-Wolf IGH. Cytokine-induced killer cells are type II natural killer T cells. *GMS Ger Med Sci.* (2007) 5:Doc07.
- Cappuzzello E, Sommaggio R, Zanollo P, Rosato A. Cytokines for the induction of antitumor effectors: The paradigm of Cytokine-Induced Killer (CIK) cells. *Cytokine Growth Factor Rev.* (2017) 36:99–105. doi: 10.1016/j.cytogfr.2017.06.003
- Verneris MR, Baker J, Edinger M, Negrin RS. Studies of ex vivo activated and expanded CD8+ NK-T cells in humans and mice. *J Clin Immunol.* (2002) 22:131–6. doi: 10.1023/A:1015415928521
- Joshi PS, Liu JQ, Wang Y, Chang X, Richards J, Assarsson E, et al. Cytokine-induced killer T cells kill immature dendritic cells by TCR-independent and perforin-dependent mechanisms. *J Leukoc Biol.* (2006) 80:1345–53. doi: 10.1189/jlb.0506305
- Liang G, Feng G, Chen H, Li L, Hu J, Zhou C, et al. Changes in the TCR repertoire of T-cell subsets during culture of cytokine-induced killer cells. *FEBS Lett.* (2022) 596:2696–705. doi: 10.1002/1873-3468.14501
- Ortaldo JR, Winkler-Pickett RT, Yagita H, Young HA. Comparative studies of CD3- and CD3+ CD56+ cells: examination of morphology, functions, T cell receptor rearrangement, and pore-forming protein expression. *Cell Immunol.* (1991) 136:486–95. doi: 10.1016/0008-8749(91)90369-M
- Merker M, Pfirrmann V, Oelsner S, Fulda S, Klingebiel T, Wels WS, et al. Generation and characterization of ErbB2-CAR-engineered cytokine-induced killer cells for the treatment of high-risk soft tissue sarcoma in children. *Oncotarget.* (2017) 8:66137–53. doi: 10.18632/oncotarget.19821
- Rettinger E, Kreyenberg H, Merker M, Kuçi S, Willasch A, Bug G, et al. Immunomagnetic selection or irradiation eliminates alloreactive cells but also reduces anti-tumor potential of cytokine-induced killer cells: implications for unmanipulated cytokine-induced killer cell infusion. *Cytotherapy.* (2014) 16:835–44. doi: 10.1016/j.jcyt.2014.01.003
- Schmidt-Wolf IGH, Negrin RS, Kiem HP, Blume KG, Weissman IL. Use of a SCID mouse/human lymphoma model to evaluate cytokine-induced killer cells with potent antitumor cell activity. *J Exp Med.* (1991) 174:139–49. doi: 10.1084/jem.174.1.139
- Pievani A, Borleri G, Pende D, Moretta L, Rambaldi A, Golay J, et al. Dual-functional capability of CD3+CD56+ CIK cells, a T-cell subset that acquires NK function and retains TCR-mediated specific cytotoxicity. *Blood.* (2011) 118:3301–10. doi: 10.1182/blood-2011-02-336321
- Yoon SH, Lee JM, Woo SJ, Park MJ, Park JS, Kim HS, et al. Transfer of her-2/neu specificity into cytokine-induced killer (CIK) cells with RNA encoding chimeric immune receptor (CIR). *J Clin Immunol.* (2009) 29:806–14. doi: 10.1007/s10875-009-9308-6
- Skapek SX, Ferrari A, Gupta AA, Lupo PJ, Butler E, Shipley J, et al. Rhabdomyosarcoma. *Nat Rev Dis Primer.* (2019) 5:41572. doi: 10.1038/s41572-018-0051-2
- De Giovanni C, Landuzzi L, Palladini A, Nicoletti G, Nanni P, Lollini PL. HER tyrosine kinase family and rhabdomyosarcoma: role in onset and targeted therapy. *Cells.* (2021) 10:1808. doi: 10.3390/cells10071808
- Ahmed N, Brawley VS, Hegde M, Robertson C, Ghazi A, Gerken C, et al. Human epidermal growth factor receptor 2 (HER2) - Specific chimeric antigen receptor - Modified T cells for the immunotherapy of HER2-positive sarcoma. *J Clin Oncol.* (2015) 33:1688–96. doi: 10.1200/JCO.2014.58.0225
- Hegde M, Joseph SK, Pashankar F, DeRenzo C, Sanber K, Navai S, et al. Tumor response and endogenous immune reactivity after administration of HER2 CAR T cells in a child with metastatic rhabdomyosarcoma. *Nat Commun.* (2020) 11:3549. doi: 10.1038/s41467-020-17175-8
- Hegde M, Navai S, DeRenzo C, Joseph SK, Sanber K, Wu M, et al. Autologous HER2-specific CAR T cells after lymphodepletion for advanced sarcoma: a phase 1 trial. *Nat Cancer.* (2024) 5:880–94. doi: 10.1038/s43018-024-00749-6
- Merker M, Wagner J, Kreyenberg H, Heim C, Moser LM, Wels WS, et al. ERBB2-CAR-engineered cytokine-induced killer cells exhibit both CAR-mediated and innate immunity against high-risk rhabdomyosarcoma. *Front Immunol.* (2020) 11:1–13. doi: 10.3389/fimmu.2020.581468
- Abel T, El Filali E, Waern J, Schneider IC, Yuan Q, Münch RC, et al. Specific gene delivery to liver sinusoidal and artery endothelial cells. *Blood.* (2013) 122:2030–8. doi: 10.1182/blood-2012-11-468579

46. Rettinger E, Meyer V, Kreyenberg H, Volk A, Kuçi S, Willasch A, et al. Cytotoxic capacity of IL-15-stimulated cytokine-induced killer cells against human acute myeloid leukemia and rhabdomyosarcoma in humanized preclinical mouse models. *Front Oncol.* (2012) 2:1–12. doi: 10.3389/fonc.2012.00032
47. Schönfeld K, Sahn C, Zhang C, Naundorf S, Brendel C, Odendahl M, et al. Selective inhibition of tumor growth by clonal NK cells expressing an erbB2/HER2-specific chimeric antigen receptor. *Mol Ther.* (2015) 23:330–8. doi: 10.1038/mt.2014.219
48. Demaison C, Parsley K, Brouns G, Scherr M, Battmer K, Kinnon C, et al. High-level transduction and gene expression in hematopoietic repopulating cells using a human immunodeficiency virus type 1-based lentiviral vector containing an internal spleen focus forming virus promoter. *Hum Gene Ther.* (2002) 13:803–13. doi: 10.1089/10430340252898984
49. Heim C, Moser LM, Kreyenberg H, Bonig HB, Tonn T, Wels WS, et al. ErbB2 (HER2)-CAR-NK-92 cells for enhanced immunotherapy of metastatic fusion-driven alveolar rhabdomyosarcoma. *Front Immunol.* (2023) 14:1228894. doi: 10.3389/fimmu.2023.1228894
50. Perez-Riverol Y, Csordas A, Bai J, Bernal-Llinares M, Hewapathirana S, Kundu DJ, et al. The PRIDE database and related tools and resources in 2019: improving support for quantification data. *Nucleic Acids Res.* (2019) 47:D442–50. doi: 10.1093/nar/gky1106
51. Segovis CM, Schoon RA, Dick CJ, Nacusi LP, Leibson PJ, Billadeau DD. PI3K links NKG2D signaling to a crkL pathway involved in natural killer cell adhesion, polarity, and granule secretion. *J Immunol.* (2009) 182:6933–42. doi: 10.4049/jimmunol.0803840
52. Hombach AA, Rappl G, Abken H. Arming cytokine-induced killer cells with chimeric antigen receptors: CD28 outperforms combined CD28–OX40 “Super-stimulation. *Mol Ther.* (2013) 21:2268–77. doi: 10.1038/mt.2013.192
53. Burger MC, Forster MT, Romanski A, Straßheimer F, Macas J, Zeiner PS, et al. Intracranial injection of natural killer cells engineered with a HER2-targeted chimeric antigen receptor in patients with recurrent glioblastoma. *Neuro-Oncol.* (2023) 25:2058–71. doi: 10.1093/neuonc/noad087
54. Rettinger E, Huenecke S, Bonig H, Merker M, Jarisch A, Soerensen J, et al. Interleukin-15-activated cytokine-induced killer cells may sustain remission in leukemia patients after allogeneic stem cell transplantation: feasibility, safety and first insights on efficacy. *Haematologica.* (2016) 101:e153–6. doi: 10.3324/haematol.2015.138016
55. Bremm M, Pfeffermann LM, Cappel C, Katzki V, Erben S, Betz S, et al. Improving clinical manufacturing of IL-15 activated cytokine-induced killer (CIK) cells. *Front Immunol.* (2019) 10:84–94. doi: 10.3389/fimmu.2019.01218
56. Stenger D, Stief TA, Kaeuferle T, Willier S, Rataj F, Schober K, et al. Endogenous TCR promotes *in vivo* persistence of CD19-CAR-T cells compared to a CRISPR/Cas9-mediated TCR knockout CAR. *Blood.* (2020) 136:1407–18. doi: 10.1182/blood.202005185
57. Morris EC, Neelapu SS, Giavridis T, Sadelain M. Cytokine release syndrome and associated neurotoxicity in cancer immunotherapy. *Nat Rev Immunol.* (2022) 22:85–96. doi: 10.1038/s41577-021-00547-6
58. Bell M, Gottschalk S. Engineered cytokine signaling to improve CAR T cell effector function. *Front Immunol.* (2021) 12:1–16. doi: 10.3389/fimmu.2021.684642
59. Laskowski TJ, Biederstädt A, Rezvani K. Natural killer cells in antitumour adoptive cell immunotherapy. *Nat Rev Cancer.* (2022) 22:557–75. doi: 10.1038/s41568-022-00491-0
60. Larson RC, Kann MC, Bailey SR, Haradhvala NJ, Llopis PM, Bouffard AA, et al. CAR T cell killing requires the IFN γ R pathway in solid but not liquid tumours. *Nature.* (2022) 604:563–70. doi: 10.1038/s41586-022-04585-5
61. Kantari-Mimoun C, Barrin S, Vimeux L, Haghiri S, Gervais C, Joaquina S, et al. CAR T-cell entry into tumor islets is a two-step process dependent on IFN γ and ICAM-1. *Cancer Immunol Res.* (2021) 9:1425–38. doi: 10.1158/2326-6066.CIR-20-0837
62. van den Elsen PJ. Expression regulation of major histocompatibility complex class I and class II encoding genes. *Front Immunol.* (2011) 2:1–9. doi: 10.3389/fimmu.2011.00048
63. Alspach E, Lussier DM, Schreiber RD. Interferon γ and its important roles in promoting and inhibiting spontaneous and therapeutic cancer immunity. *Cold Spring Harb Perspect Biol.* (2019) 11:a028480. doi: 10.1101/cshperspect.a028480
64. Moesta AK, Li XY, Smyth MJ. Targeting CD39 in cancer. *Nat Rev Immunol.* (2020) 20:739–55. doi: 10.1038/s41577-020-0376-4
65. Simoni Y, Becht E, Fehlings M, Loh CY, Koo SL, Teng KWW, et al. Bystander CD8+ T cells are abundant and phenotypically distinct in human tumour infiltrates. *Nature.* (2018) 557:575–9. doi: 10.1038/s41586-018-0130-2
66. Canale FP, Ramello MC, Núñez N, Araujo Furlan CL, Bossio SN, Gorosito Serrán M, et al. CD39 expression defines cell exhaustion in tumor-infiltrating CD8+ T cells. *Cancer Res.* (2018) 78:115–28. doi: 10.1158/0008-5472.CAN-16-2684
67. Duhon T, Duhon R, Montler R, Moses J, Moudgil T, de Miranda NF, et al. Co-expression of CD39 and CD103 identifies tumor-reactive CD8 T cells in human solid tumors. *Nat Commun.* (2018) 9:2724. doi: 10.1038/s41467-018-05072-0
68. Kang G, Zhao X, Sun J, Cheng C, Wang C, Tao L, et al. A2AR limits IL-15-induced generation of CD39+ NK cells with high cytotoxicity. *Int Immunopharmacol.* (2023) 114:109567. doi: 10.1016/j.intimp.2022.109567
69. Yan J, Li XY, Roman Aguilera A, Xiao C, Jacobberger-Foissac C, Nowlan B, et al. Control of metastases via myeloid CD39 and NK cell effector function. *Cancer Immunol Res.* (2020) 8:356–67. doi: 10.1158/2326-6066.CIR-19-0749
70. Walker LSK, Sansom DM. The emerging role of CTLA4 as a cell-extrinsic regulator of T cell responses. *Nat Rev Immunol.* (2011) 11:852–63. doi: 10.1038/nri3108
71. Tian M, Wei JS, Shivaprasad N, Highfill SL, Gryder BE, Milewski D, et al. Preclinical development of a chimeric antigen receptor T cell therapy targeting FGFR4 in rhabdomyosarcoma. *Cell Rep Med.* (2023) 4:101212. doi: 10.1016/j.xcrm.2023.101212
72. Ahmed N, Salsman VS, Yvon E, Louis CU, Perlaky L, Wels WS, et al. Immunotherapy for osteosarcoma: genetic modification of T cells overcomes low levels of tumor antigen expression. *Mol Ther.* (2009) 17:1779–87. doi: 10.1038/mt.2009.133
73. Duncan BB, Dunbar CE, Ishii K. Applying a clinical lens to animal models of CAR-T cell therapies. *Mol Ther - Methods Clin Dev.* (2022) 27:17–31. doi: 10.1016/j.jomtm.2022.08.008
74. Page A, Chuvin N, Valladeau-Guilemond J, Depil S. Development of NK cell-based cancer immunotherapies through receptor engineering. *Cell Mol Immunol.* (2024) 21:315–31. doi: 10.1038/s41423-024-01145-x